Flashback and Blowoff Stability Analysis of Hydrogen Enriched Natural Gas using Bunsen Flames

Diogo Filipe de Deus Vozone
diogovozone@tecnico.ulisboa.pt

Instituto Superior Técnico, Universidade de Lisboa, Portugal

October 2021

Abstract

In this work, the impacts of hydrogen enrichment of natural gas in fundamentals combustion aspects such as the flashback and blowoff phenomena in Bunsen Flames were studied. At the same time, dimensional analysis was used to predict the onset of flame flashback and also applied particle image velocimetry techniques on the isothermal flow field to verify whether the underlying assumptions typically made on the study of critical velocity gradients were valid. Six fuel mixtures from pure methane, NG100, to NG60 H40, 3 different diameters, 7mm, 10mm and 14mm and 6 different equivalence ratios from 0.8 to 1.3, were used in the experiments. Two equations describing the variation of the critical velocity gradients for natural gas with hydrogen percentage xH_2 and equivalence ratio ϕ were suggested. Regarding the operation limits of a Bunsen burner, the optimum diameters and ranges of admissible flows were presented in the form of Glassman diagrams and analysed for with highest hydrogen content accepted in Portugal taking into account the Wobbe Index. The dimensional analysis showed good results when interpolating the results of flashback data, providing evidence that "K" is not in fact a constant, but varies significantly with different mixtures used. Taking the values of K obtained, the mixture NG90 H10 would be the least susceptible to flashback while the mixture NG60 H40 would be the most susceptible to flashback. The measured velocity profiles comparison against the calculated velocity profiles showed that the assumption of Poiseuille flow can provide non realistic values when calculating blowoff critical velocity gradients.

Keywords: flashback, blowoff, Bunsen flame, hydrogen, natural gas

1. Introduction

Climate change is one of the main causes for global concern, reflected in the rise of global temperature, extreme weather events, drought, biodiversity and more. Eighty to ninety percent of natural disasters in the last 10 years are due to floods, droughts and severe storms and two hundred and fifty thousand additional deaths are expected to happen from climate-sensitive diseases from 2030 onward [11].

Engineering and science in general play a big role on overcoming these hard challenges. Particularly, the study of mechanical engineering and combustion has the possibility of changing the next decades' path towards a greener and more sustainable society. It is of the utmost importance to come up with viable solutions that are compatible with this decade's demands without compromising the current standards of living.

Hydrogen can be a key part in the complex energy system worldwide and specifically, in Portugal. This way, this thesis is focused on improving the knowledge around the topic and, in more detail, complementing the existing literature on hydrogen enrichment of natural gas and its potential in Portugal in the upcoming years.

"Hydrogen at Scale concept" [14], proposes hydrogen as a third energy infrastructure, joining the electric grid and the natural gas infrastructure. On the generation side, hydrogen can be produced using various conventional and renewable energy sources. On the application side, hydrogen has many current and possible future applications across the sectors of transportation, chemical and industrial processes, fertilisers and heat production.

In fact, the European Hydrogen Strategy, launched by the European Commission, aims to install a capacity of 40 GW of green hydrogen production until 2030, contributing to make Europe the first carbon neutral continent. Also, the share of hydrogen in Europe's energy mix is projected to grow from the current less than 2% to 13-14% by 2050 [2].

In the Portuguese context there are also goals and objectives regarding the implementation of green hydrogen in the country. The following goals have been set to attain by the year 2030: injection of

10%-15% of H_2 in the natural gas network, 2%-5% H_2 in the industry consumption as also projects to increase the production capacity of green hydrogen to a total of around 2.5 GW [13].

1.1. Combustion of Premixed Flames

Bunsen burners are used to obtain laminar premixed flames, which main characteristics are a relatively high temperature, a blue flame with low radiation and no soot emissions. Many household, commercial, and industrial equipment and processes use laminar premixed flames, which are often used in conjunction with diffusion flames.

The laminar flame speed is an important parameter of a combustible mixture. The value of the flame speed has important effects upon the propensity of the flame to flashback and blowoff, and it also controls other key combustion characteristics, such as the flame's spatial distribution [3].

Some of the factors influencing flame speed are the temperature of the reactants, equivalence ratio, pressure, flame curvature and flame temperature. The temperature of the reactants was a special concern in this work since other authors such as Lewis and Von Elbe and students previously working in similar setups in this laboratory reported high tube temperatures that would definitely impact the downstream flow, and consequently the flame speed.

Experimental data for hydrocarbon flames burning in air show that the laminar flame speed changes with the temperature of the reactants according to:

$$S_L \propto T_o^m \tag{1}$$

with m ranging between 1.5 and 2.0.

Equivalence ratio is another factor influencing the burning velocity of flames. It can be defined as the ratio of the fuel mass flow rate to the air mass flow rate divided by the same ratio at the stoichiometry of the reaction considered [12].

Given the fact that the adiabatic flame temperature is a function of the equivalence ratio and since the maximum adiabatic flame temperature, in the case of hydrocarbons, reaches a maximum at $\phi = 1$ or slightly higher than 1, the same happens with the burning velocity.

The peak of S_L shifts to $\phi = 1.8$ for hydrogen due to the substantial increase of the thermal diffusivity with equivalence ratio ϕ. At a temperature of T = 298 K and pressure P = 1 atm, the values for the laminar flame speed of hydrogen (H_2), methane (CH_4) and propane (C_3H_8) are 219.7 cm/s, 36.2 cm/s and 46.3 cm/s, respectively [5]. Hydrogen has a higher laminar flame speed than the hydrocarbons due its higher thermal diffusivity.

The other two important flame phenomena to introduce are the phenomena of flame flashback and flame blowoff and these are both related to equilibrium between the mass flow rate of the mixture and the local burning velocity.

If the velocity of the mixture exceeds the laminar flame speed, the flame front will move in the same direction as the mixture, towards the burner exit. The other way around, if the laminar flame speed exceeds the velocity of the mixture, the flame will propagate upstream into the tube, which could potentiate security problems.

1.2. Interchangeability of Gaseous Fuels

The Wobbe Index, WI, is the standard measurement of interchangeability between gaseous fuels. Regardless of calorific value, gases with the same WI produce the same heat load in a gas burner. Therefore WI is by far the most important combustion parameter for gas appliances. [1].

The Wobbe Index [MJ/Nm^3] is normally defined as [6]:

$$WI = \frac{HHV}{\sqrt{SG}} \tag{2}$$

where HHV [MJ/Nm^3] is the higher heating value, and SG is the specific density of the gas compared to air, dimensionless.

Wobbe Index values for natural gas vary according to its specific composition, but a value of 51MJ.Nm^{-3} may be taken as a characteristic lower bound for natural gas supplied with several European countries [7], while a value of WI = 48.6MJ.Nm^{-3} may be assumed for hydrogen. In the scope of this work it is interesting to analyse how the index varies with the addition of hydrogen to natural gas, and this is the information shown in Fig. 1.

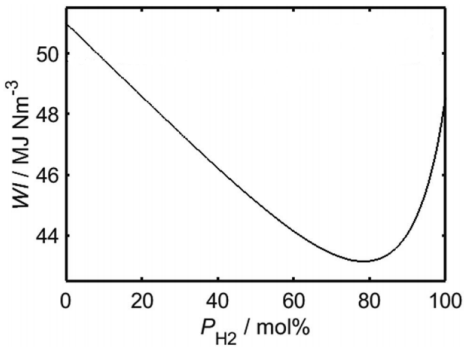

Figure 1: Variation of the Wobbe Index as a function of molar hydrogen percentage in HENG. Adapted from [7]

With the graph above in mind, it is interesting to note that nowadays, in Portugal, the range of accepted values of Wobbe Index by national regulation is between 49.43MJ.Nm^{-3} and 52.76MJ.Nm^{-3}

[16], which doesn't seem to permit percentages of hydrogen any higher than 20%, strictly looking into the Wobbe Index information.

1.3. State of the Art

In 1943, Bernard Lewis and Guenther von Elbe publish the work "Stability and Structure of Burner Flames" [9] in which it is proposed the concept of critical velocity gradient g_c.

This velocity gradient concept is traditionally used to describe the phenomena of blowoff and flashback and is based on the laminar jet flame's tendency to propagate upstream or downstream when the laminar burning velocity exceeds or subceeds the local flow velocity. It is also mentioned by Lewis and von Elbe that the critical velocity gradient for flashback "is obviously determined solely by factors that affect the burning velocity near the wall, namely, the condition of the wall (temperature mainly) and the mixture composition".

The proposed gradient,

$$g_{\mathrm{F,B}} \equiv -\lim_{r \to R}(du/dr) \tag{3}$$

is explored for different natural gas-air mixtures and tube diameters. The authors also report that the results are affected by the increase in tube temperatures up to about 100 ºC, in glass tubes.

Different dimensionless approaches have been suggested, including using "Damköhler numbers" Da (ratio of reaction timescale to the convection time scale) as a flashback propensity indicator and using "Peclet numbers" Pe. The latter is the approach suggested by Putnam and Jensen [15].

Putman and Jensen proposed that the onset of flashback may be defined by the "Peclet numbers" Pe_F (flame Peclet number) and Pe_J (jet Peclet number):

$$Pe_F = \frac{2RS_L c_p \rho}{\lambda} \tag{4}$$

$$Pe_J = \frac{2Ru_{av} c_p \rho}{\lambda} \tag{5}$$

where R is the tube radius, S_L is the laminar flame speed, c_p the specific heat at constant pressure, ρ the density, λ the coefficient of thermal conductivity and u_{av} is the average jet velocity.

In a more recent work, 2015, Duan and McDonell [4] selected the critical Damköhler number as the indicator of flashback propensity. The authors developed an empirical physical model for flashback propensity as a function of dimensionless groups.

The potential variables determining flashback behaviour where catalogued into five types: operational parameters, unburnt conditions, ambient conditions, rig properties, and others. An extensive list of parameters determining flashback behaviour is presented and another list with the respective relations among the listed parameters. Furthermore, the Buckingham Pi theorem was used to conduct a dimensional analysis that resulted in the following expression for the critical Damköhler number [4]:

$$Da = \text{ Const. } \cdot Le^{-6.12} \cdot \left(\frac{T_u}{T_0}\right)^{-1.71} \cdot \left(\frac{T_{tip}}{T_u}\right)^{-3.69}$$

$$\mathrm{P\ e}_f^{1.89} \cdot f_1\left(\frac{\theta'}{d}\right) \cdot f_2\left(\frac{P_u}{P_0}\right) \tag{6}$$

This model suggests a concrete significance of various parameters such as preferential diffusion (Le), heat loss ($\frac{T_u}{T_0}$), thermal coupling effect ($\frac{T_{tip}}{T_u}$) and flame Peclet number (Pe_f). Higher Damköhler number Da values indicate less mass flow is required to avoid flashback, i.e. greater flashback resistance.

The work of Jones and Dunnill [7] focuses on the practical challenges ahead when considering the hydrogen enrichment of domestic natural gas in the United Kingdom. The physical properties of hydrogen make it impossible to simply interchange the two gases without a major overhaul of the existing energy network [7]. It is essential to ensure that neither flashback or blowoff could occur during a changeover from natural gas to HENG.

It has been shown by the authors that whilst hydrogen-enrichment acts to lower the calorific value of natural gas, it also augments the stability of a burner by suppressing the occurrence of flame blowoff and prevents yellow tipping by lowering the oxygen-requirements of the fuel.

It is also concluded that for ports less than 3.5mm in diameter, HENG fuel containing as much as 50 mol% hydrogen may be ignited safely without risk of flashback while flashback upon extinction of the flame occurs only if the hydrogen proportion exceeds approximately 34.7 mol%.

Jones and Dunnill end the work by mentioning that to properly evaluate the virtues and shortcomings of a given proposed composition of hydrogen-enriched natural gas, quantifying the physical effects of hydrogen-enrichment as a function of hydrogen percentage is a critical first step.

2. Experimental Work

2.1. Flame stability test

The laboratory setup used for the stability tests has the goal of visualising the occurrence of both flame flashback and blowoff in a Bunsen burner using a simple setup of gas bottles (CH_4 and H_2) and compressed atmospheric air, connected through security valves and flow meters to a mixing chamber. These are connected to the Bunsen burners via a 3D printed adaptors. The metallic area of this set (tube plus adaptor) is cooled using a cooling sleeve designed for the purpose, which uses flowing water as a cooling liquid controlled also by a flow meter.

All the flow meters are controlled by a GUI in LabView through a computer.

The Bunsen tubes consisted of 3 Stainless Steel (ANSI 304) tubes with the diameters of 7 mm, 10 mm and 14 mm and a wall thickness of 1 mm. Each tube's length was chosen to guarantee that the flow was fully developed and the streamlines were as undisturbed as possible after the mixing chamber and the quenching net.

The data points regarding the flame stability experiments were obtained directly through the Bunsen tubes setup. The tests performed consisted in inducing both flashback and blowoff to a stable flame. This was achieved, in the former, through a consistent decrease in flow rate (small steps of Re), while keeping the composition constant, until the flame is unable to stabilise itself and enters the tube. The same approach was taken to blowoff tests, using Re changes in the opposite direction, i.e. through a consistent increase in the mixture flow rate until the flame is lifted and "leaves" the Bunsen tube.

To follow the Glassman's diagram methodology presented in [5], "critical velocity gradients" for flashback and blowoff must be calculated. This gradient is defined as:

$$g_{\mathrm{F,B}} \equiv -\lim_{r \to R}(du/dr) \tag{7}$$

$$g_{\mathrm{F,B}} = \frac{8}{d} u_{av} = \frac{8\nu}{d^2}\mathrm{Re} \tag{8}$$

To obtain the singular values for the gradients $g_{\mathrm{F,B}}$ needed to compute the Glassman's diagram, an average of each three values (three diameters) was taken.

2.2. Particle Image Velocimetry

The laboratory setup for the Particle Image Velocimetry (PIV) tests was assembled with the goal of obtaining cross sectional velocity profiles at the exit of the Bunsen burner tubes. This enables us to evaluate to some degree the suitability of the critical velocity gradients calculated using Eq. 8.

The setup is composed of the same setup used in the flame stability tests presented in Section 2.1, without the water cooling sleeve and water supply, and additionally using a laser, camera, synchronizer, seeding flask with tracer particles and a magnetic stirrer.

A two phase approach was taken in the experiments to obtain the velocity profiles at the Bunsen tubes exits.

A a first phase had the goal of creating a "baseline" to work with for the second phase. This means comparing in isothermal conditions (no flame) the velocity profiles obtained when the studied mixture was pure air with the velocity profiles obtained from experiments using only CH_4 (NG 100) and the natural gas mixture with the highest xH_2 (NG60 H40). If the profiles overlap sufficiently such that they could be interchangeable, for the second phase only air flow is necessary to simulate the results obtain with the other mixtures.

The second phase consisted in using air as the fluid in study and selecting flow conditions that, if a combustible mixture were used with a flame, produce instability events such as flashback and blowoff, in all the diameters under study. The flow velocities, i.e. Reynolds numbers, were chosen taking into account the data from the flame stability tests to be representative of both the flashback and blowoff regions.

3. Results

3.1. Influence of H_2 enrichment of Natural Gas on flashback and blowoff stability limits

For flame stability experiments, the six mixtures studied, range of mixture equivalence ratios, tube diameters and other operating conditions are represented in Table 1.

Table 1: Operational conditions used for flashback and blowoff stability experiments.

Hydrogen enrichment, xH_2[%]	0, 5, 10, 20, 30, 40
Equivalence ratio, ϕ	0.8, 0.9, 1.0, 1.1, 1.2, 1.3
Bunsen tube diameter [mm]	7, 10, 14
Cooling water flow rate [slpm]	0.2

The critical velocity gradients obtained are shown in graphs $g_F = f(\phi)$ and $g_B = f(\phi)$ of Fig. 2 and compile the information from the three tube diameters resulting in an unique value for each fixed mixture and equivalence ratio ϕ.

Positive values of g_F and g_B as observed indicate that the average flow velocity at which flashback and blowoff occur increases with the tube's diameters. This is found in accordance with results found in the literature [15, 10, 8].

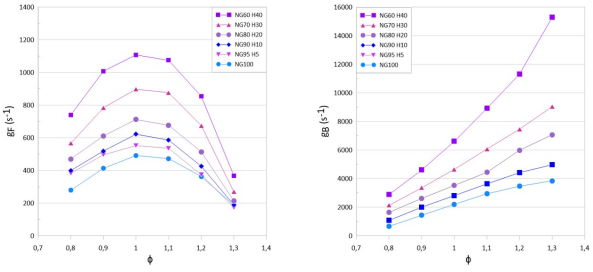

Figure 2: Flashback and blowoff critical velocity gradients for different mixtures of Natural Gas and Hydrogen

The impact on the curves when adding hydrogen is noticeable and pronounced, specially when 20% H_2 or more is used as a mixture. For the flashback curves on the left, critical velocity gradients range from value of 200 s^{-1} to 1100 s^{-1}, exhibiting the maximum values at about stoichiometric conditions for every mixture and the highest values overall for NG60 H40.

The blowoff limits show similar results, with critical velocity gradients ranging from 650 s^{-1} to about 15000 s^{-1}. A pronounced impact is found on the stability of the flames when adding more than 30% H_2 as the NG60 H30 shows a higher parabolic increase for richer mixtures. All the mixtures studies provided a maximum stability against blowoff for the richest equivalence ratio ϕ=1.3, as expected.

A parametric description for the variation of the flashback and blowoff gradients with hydrogen percentage xH_2 and equivalence ratio ϕ is suggested:

$$g_F(xH_2,\phi) = (-127xH_2 - 3807)(\phi^2) + (257\text{x}H_2 + 7729)(\phi) + (-114xH_2 - 3461)[s^{-1}] \quad (9)$$

$$g_B(xH_2,\phi) = (249xH_2 + 6036)(\phi) + (\text{-}160\text{x}H_2 - 4050)[s^{-1}] \quad (10)$$

3.2. Influence of H_2 enrichment of Natural Gas on the operation limits of a Bunsen Burner

When considering the design of Bunsen tubes and cooking stoves that use gaseous fuels, the importance of understanding stability limits becomes very clear. The maximum range of volumetric flow without experiencing stability concerns is desirable in the construction of a Bunsen burner.

With the goal of understanding the impact of H_2 enrichment in the operation of burners, the graphs $\bar{u}_v = f(d)$ shown in Fig. 3 were put together. The dashed area represents the region that has the greatest flow variability without stabilisation problems.

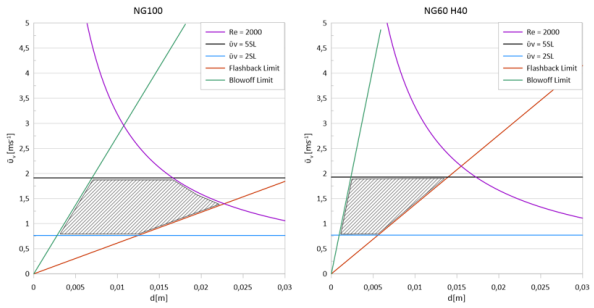

Figure 3: Operational area of Bunsen burners for different mixtures (ϕ=1)

The range variation of admissible flows $\bar{u}_v$ observed in this case is negligible, since values of $\bar{u}_v = f(d)$ between 0.75 ms^{-1} and ~1.9 ms^{-1} offer the maximum range in all mixtures. For the case of only natural gas (NG100) values of diameters between d = 7.5mm and d=12mm seem to provide the maximisation of the dashed area without stability issues. Furthermore, a decrease in this area is considerable in the mixture with 40% H_2, in which the maximisation of the dashed stable area happens for diameters between d = 2mm and d = 6mm.

3.3. Dimensional Analysis

The approach suggested by Putnam and Jensen [15] will be applied here and verified its applicability to the flashback data sets.

The authors suggested that the flashback propensity of a given fuel could be approximated using the relationship between the two "Peclet numbers":

$$Pe_J = \frac{1}{8K}(Pe_F)^2 \quad (11)$$

where K is a fuel-dependent constant and the final approximation holds when K/P_F is much less than one.

To test the theory proposed with the present flashback data, the square dependency of Eq. 11 and the variation of the constant K with different mixtures can be analysed.

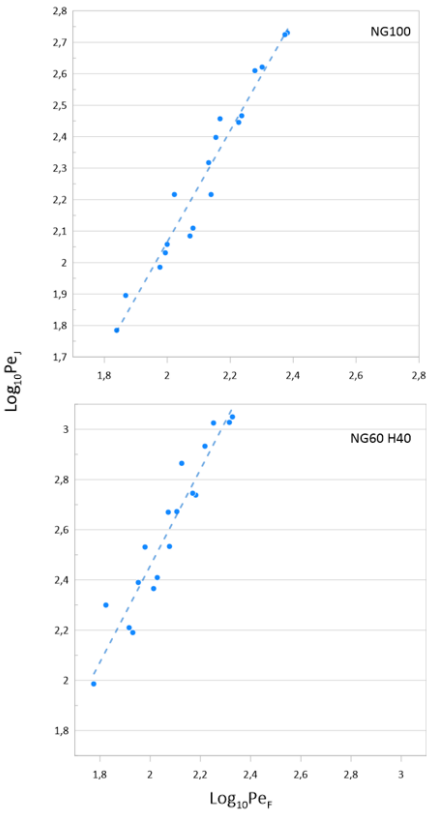

Figure 4: Scatter plots and respective linear regressions of logarithmic Peclet numbers for different mixtures

Applying logarithms to Eq. 11 one obtains:

$$\log_{10}(\mathrm{Pe_J}) = \log_{10}(1/8\mathrm{K}) + 2\log_{10}(\mathrm{Pe_F}) \quad (12)$$

It is now possible to plot this equation applied to the data collected for flashback instabilities and obtain a scatter plot. This scatter plot may follow a linear trend line of the form:

$$\log_{10}(\mathrm{Pe_J}) = b + a\log_{10}(\mathrm{Pe_F}) \quad (13)$$

in which the constant "a" will be taken as the slope of the linear polynomial and will be compared to the square dependency suggested in theory, and the constant "b" will be taken as the value of the linear polynomial in xx=0 and will result in the constant "K" by calculating : $K = \left(10^{-b}\right)/8$.

Table 2: Linear polynomial regressions constants and coefficient of determination of graphs in Fig. 4

Mix	a	b	K	R^2
NG100	1.7678	-1.4697	3.68	0.9526
NG95 H5	1.832	-1.5515	4.45	0.8914
NG90 H10	1.9319	-1.7242	6.62	0.8903
NG80 H20	1.9341	-1.6511	5.59	0.8952
NG70 H30	1.9054	-1.4761	3.74	0.9047
NG60 H40	1.9194	-1.3827	3.01	0.9095

The high values (around ∼0.9) of the coefficient of determination R^2 shows that the linear polynomial is in fact a good model to describe the present data and provide sufficient reliability to the following analysis.

The slope "a" is found to be in the range of values between 1.7678 and 1.9341, with an average of 1.88. These are in average only 5.9% smaller than the suggested a=2 in theory, and only the mixture NG100 exhibits a slightly bigger deviation than would be wished.

In order to assess the impact the variation in the constant K has on the onset of flashback, both Eq. 14 and the graph in Fig. 5 can be useful:

Equation 11 can be re-written to take the form:

$$u_{\mathrm{av}} = \frac{{S_\mathrm{L}}^2 d_{\mathrm{port}}}{8K\alpha} \quad (14)$$

which allows the onset of flashback to be predicted across a range of u_{av} values.

It is a consequence of these that increasing the magnitude of K results in a decrease in the value of u_{av} for a given S_L, thereby lowering the susceptibility of the system to flashback. Taking this into consideration, and the values of K obtained, the mixture NG90 H10 would be the least susceptible to flashback while the mixture NG60 H40 would be the most susceptible to flashback, with K values of 6.62 and 3.01, respectively.

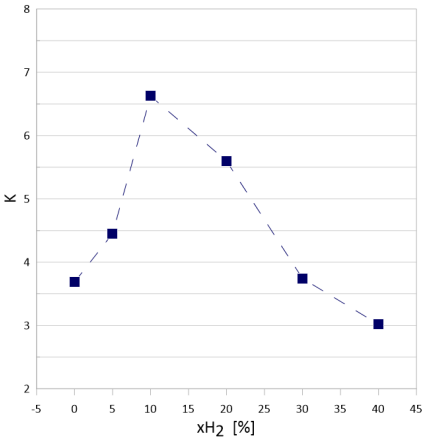

Figure 5: Variation of the constant K with change in hydrogen molar percentage in a HENG mixture

3.4. Velocity profiles and flow field - PIV

The first phase had the goal of comparing, in isothermal conditions (no flame), the velocity profiles obtained when the studied mixture was pure air with the velocity profiles obtained from experiments using only CH_4 (NG 100) and the natural gas mixture with the highest xH_2 (NG60 H40). For this comparison to be valid, all the other variables were kept fixed such as the Reynolds number and tube diameter.

Table 3: Detailed approach and conditions under which phase one of PIV analysis was performed

	Mix	Re	ϕ
	Air	500	-
1st Phase	**NG 100**	500	1
(d=10 mm)	**NG60 H40**	500	1

For this purpose, the three mixtures mentioned were tested in the 10mm diameter Bunsen tube, a Reynolds number of Re = 500 (providing laminar flow test conditions) and an equivalence ratio of $\phi = 1$ for the two combustible mixtures, NG100 and NG60 H40.

In Fig. 6 the plots of the three different velocity profiles obtained are presented in the form of a $V = f(x)[m/s]$ where x represents the distance between 0 and R or $-R$ millimetres from the axis of

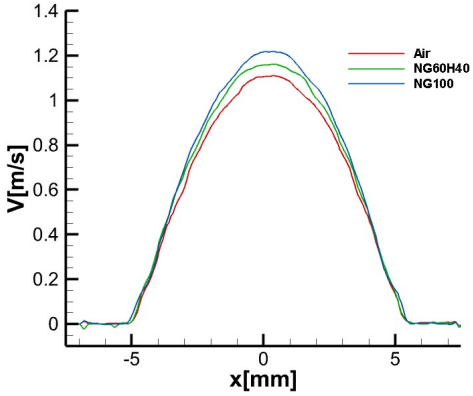

Figure 6: Velocity profiles at the end of Bunsen tubes for Re=500 and d=10mm for different mixtures

the tube. The three profiles have a parabolic shape and it can be observed some velocity difference in the vicinity of $x = 0mm$ which can be explained by the different specific masses of the three mixtures and this being the region with the highest velocities, making these differences more impact-full. However, since the approach taken is intended to verify the usability of critical velocity gradients

$$g_{\mathrm{F,B}} \equiv -\lim_{r \to R}(dV/dx)$$

the differences in the centerline can be disregarded and the focus be put in the $\lim_{r\to R}(dV/dx)$. In this region, the three profiles actually overlap almost completely as can be seen as the limits $\lim_{r\to -5}(dV/dx)$ and $\lim_{r\to 5}(dV/dx)$ are the same in the plots shown.

The second phase of the PIV experiments had the goal of extracting the real velocity profiles of flows with Reynolds numbers that were significant to the study and comparing them with the expected theoretical velocity profiles for a Poiseuille flow.

Using air as the studied fluid, three (3) diameters were used with eight (8) Reynolds numbers for each diameter, accounting for a total of twenty four (24) PIV acquisitions performed in this phase. These conditions are detailed in Table 4 and Table 5.

Table 4: Detailed approach and conditions under which phase two of PIV analysis was performed

	Diam.	Flashback Region
	7 mm	Re = 100, 200, 300, 400
2nd Phase	**10 mm**	Re = 400, 500, 600, 800
(Air)	**14 mm**	Re = 500, 650, 780, 900

Table 5: Detailed approach and conditions under which phase two of PIV analysis was performed

	Diam.	Blowoff Region
	7 mm	1000, 1500, 2000, 2500
2nd Phase	**10 mm**	1500, 2500, 3500, 4500
(Air)	**14 mm**	1350, 1850, 2230, 2500

In Fig. 7, Fig. 8 and Fig. 9, six velocity profiles are presented that were chosen to be representative of the results obtained and the most clear to analyse. In each plot the black dots represent the velocity distribution of the stream of air at the orifice of the Bunsen measured experimentally and the black lines represents the calculated velocity distribution.

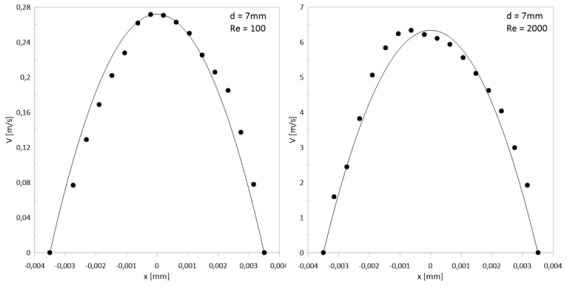

Figure 7: Velocity distribution in streams of air of different Reynolds numbers and tube diameters. Measured velocity and calculated velocity and d=7mm

Analysing the smallest diameter of 7mm, all the velocity profiles measured experimentally obtained very close results to the calculated velocity distribution, exhibiting a parabolic shape, even when Re = 2000 was reached and turbulent region was attained.

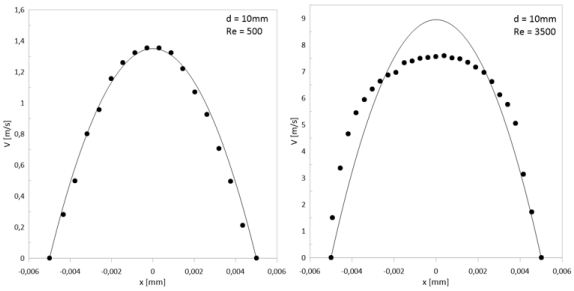

Figure 8: Velocity distribution in streams of air of different Reynolds numbers and tube diameters. Measured velocity and calculated velocity and d=10mm

When the tube in study had the diameter of

10mm, both Re = 500 and Re = 1500 velocity distribution profiles appear to follow the Poiseuille flow profile very close. However, in the second profile presented, as in some cases in the biggest tube, the velocity profiles did not approximate as well to the calculated velocity distribution and a "flattened" velocity profile was observed, with a non parabolic shape to it. This is the case of Re = 3500 presented, in which very turbulent conditions were observed.

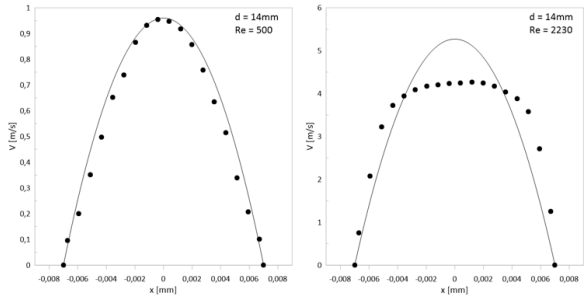

Figure 9: Velocity distribution in streams of air of different Reynolds numbers and tube diameters. Measured velocity and calculated velocity and d=14mm

Lastly, for the largest tube with a diameter of 14mm, the velocity distributions only overlap sufficiently the calculated velocity distribution up to Re = 1000. As can be seen by the highest Reynolds shown here, Re = 2230, the profiles get more and more "flattened" as the air flow is increased. Nonetheless, the more laminar flows, here represented by Re = 500, still maintain a mostly parabolic shape that overlaps the Poiseuille flow profile plotted in the black line.

4. Conclusions

The main conclusions drawn from the work developed were:

The mixture with highest hydrogen content reached flashback instabilities relatively sooner than the natural gas. For stoichiometric conditions, d = 10mm, the natural gas reached instability at Re=400, while adding a percentage of xH_2=40% caused the instability to happen at Re=830

The mixtures with higher hydrogen content only reached blowoff instability when increasing the flow rate much later than the mixtures without or with lower hydrogen content. For stoichiometric conditions, d = 10mm, the flames left the Bunsen tube at Re=1650 and Re=5115.

In none of the flashback tests the Reynolds number exceeded a value of 850. This means in all these cases the flow was laminar, while for most of the blowoff tests, specially for richer mixtures, the flows exhibited high turbulence reaching Reynolds numbers up to 7500.

The impact on the critical velocity gradients when adding hydrogen was noticeable and pronounced, specially when 20% H_2 or more was used. For the flashback curves critical velocity gradients ranged from value of 200 s^{-1} to 1100 s^{-1}, exhibiting the maximum values at about stoichiometric conditions for every mixture and the highest values overall for NG60 H40.

The blowoff limits showed similar results, with critical velocity gradients ranging from 650 s^{-1} to about 15000 s^{-1}. A pronounced impact is found on the stability of the flames when adding more than 30% H_2. All the mixtures studies provided a maximum stability against blowoff for the richest equivalence ratio ϕ=1.3.

Regarding the operation limits of a Bunsen burner, values of $\bar{u}_v = f(d)$ between 0.75 ms^{-1} and 1.9 ms^{-1} seemed to offer the maximum range in all stoichiometric mixtures. In the case of NG100 values of diameters between d = 7.5mm and d=12mm seem to provide the maximisation of the operational area without stability issues. Furthermore, a decrease in this area was considerable in both the mixtures NG90 H10 and NG70 H30, as well as in the mixture with 40% H_2, in which the maximisation of the operational stable area happens for diameters between d = 2mm and d = 6mm.

In one hand, the range variation of admissible flows $\bar{u}_v$ observed in this case is negligible, since values of $\bar{u}_v = f(d)$ between 0.75 ms^{-1} and 1.9 ms^{-1} offer the maximum range in all mixtures. On the other hand, and taking into consideration that the best burner diameter is the one that allows for a higher range of admissible flows, the differences in blowoff and flashback limits contribute to a displacement to smaller diameters. For the case of only natural gas (NG100) values of diameters between d = 7.5mm and d=12mm seem to provide the maximisation of the dashed area without stability issues. Moreover, a decrease in this area is considerable in both the mixtures NG90 H10 and NG70 H30, as well as in the mixture with 40% H_2, in which the maximisation of the dashed stable area happens for diameters between d = 2mm and d = 6mm.

When the mixture with highest hydrogen content accepted in Portugal taking into account the Wobbe Index was analysed, NG80H20, the equivalence ratio that provided a greater range of admissible flows was ϕ=1, while the leanest and richest compositions offered the smallest range. The former shows values of $\bar{u}_v = f(d)$ between 0.75 ms^{-1} and 1.9 ms^{-1} while the latter show a reduction of 47% to values of $\bar{u}_v = f(d)$ between 0.5 ms^{-1} and 1.1 ms^{-1}.

For a equivalence ratio ϕ=1.3 the dashed area occupied the range between d $\sim$ 1mm and d $\sim$ 30mm, while in the leanest mixture of equivalence ratio

ϕ=0.8 only values between d = 5mm and d = 7mm are advisable to be used in the design of Bunsen burners using NG80 H20 as a gaseous fuel.

The dimensional analysis model showed good results when interpolating the results of flashback data, providing evidence that K is not in fact a constant, but varies significantly with different mixtures used. Taking the values of K obtained, the mixture NG90 H10 would be the least susceptible to flashback while the mixture NG60 H40 would be the most susceptible to flashback, with K values of 6.62 and 3.01, respectively.

The measured velocity profiles comparison against the calculated velocity profiles showed that the critical velocity gradients assumption of Poiseuille flow used typically can provide non realistic values when calculating blowoff critical velocity gradients, but for flashback velocity gradients typical Reynolds numbers, the measured velocity profiles overlap significantly with the calculated ones, making this a trustworthy assumption.

References

[1] K. Altfeld and D. Pinchbeck. Admissible hydrogen concentrations in natural gas systems. *Gas Energy*, 2103(03):1–2, 2013.

[2] E. Commission. A hydrogen strategy for a climate-neutral europe, July 2020.

[3] C. Dong, Q. Zhou, Q. Zhao, Y. Zhang, T. Xu, and S. Hui. Experimental study on the laminar flame speed of hydrogen/carbon monoxide/air mixtures. *Fuel*, 88(10):1858–1863, 2009.

[4] Z. Duan, A. Kalantari, and V. McDonell. Parametric analysis of flashback propensity with various fuel compositions and burner materials. In *Turbo Expo: Power for Land, Sea, and Air*, volume 56697, page V04BT04A048. American Society of Mechanical Engineers, 2015.

[5] I. Glassman, R. A. Yetter, and N. G. Glumac. *Combustion*. Academic press, 2014.

[6] D. Haeseldonckx and W. D'haeseleer. The use of the natural-gas pipeline infrastructure for hydrogen transport in a changing market structure. *International Journal of Hydrogen Energy*, 32(10-11):1381–1386, 2007.

[7] D. R. Jones, W. A. Al-Masry, and C. W. Dunnill. Hydrogen-enriched natural gas as a domestic fuel: an analysis based on flash-back and blow-off limits for domestic natural gas appliances within the uk. *Sustainable Energy & Fuels*, 2(4):710–723, 2018.

[8] P. Kurz. Some factors influencing stability limits of bunsen flames. *Combustion and Flame*, 1(2):162–178, 1957.

[9] B. Lewis and G. von Elbe. Stability and structure of burner flames. *The Journal of Chemical Physics*, 11(2):75–97, 1943.

[10] D. Mishra. Experimental studies of flame stability limits of cng–air premixed flame. *Energy conversion and Management*, 48(4):1208–1211, 2007.

[11] W. H. Organization. Health topics.

[12] P. Palies. Stabilization and dynamic of premixed swirling flames: Prevaporized, stratified, partially, and fully premixed regimes. 2020.

[13] A. A. para a energia. Estratégia nacional para o higrogénio, Agosto 2020.

[14] B. Pivovar, N. Rustagi, and S. Satyapal. Hydrogen at scale (h2@ scale): key to a clean, economic, and sustainable energy system. *Electrochemical Society Interface*, 27(1):47, 2018.

[15] A. A. Putnam and R. A. Jensen. Application of dimensionless numbers to flash-back and other combustion phenomena. In *Symposium on Combustion and Flame, and Explosion Phenomena*, volume 3, pages 89–98. Elsevier, 1948.

[16] T. Williams. European gas interchangeability. In *World Gas Conference*, 2009.